Article

Improvement of Extraction Efficiency and Metabolites of Pollutants from Medium and Low Concentration Organic Polluted Soil

Xiaojuan Bai [1,2,*], Wei Song [2], Linlong Guo [2], Rujiao Liu [2], Yihan Cao [2], Pin Jin [2], Bowen Zhu [1,2] and Xiaoran Zhang [1,2]

[1] Centre for Urban Environmental Remediation, Beijing University of Civil Engineering and Architecture, Beijing 100044, China
[2] Beijing Energy Conservation & Sustainable Urban and Rural Development Provincial and Ministry Co-Construction Collaboration Innovation Center, Beijing University of Civil Engineering and Architecture, Beijing 100044, China
* Correspondence: baixiaojuan@bucea.edu.cn or heixia.1986@163.com
Received: 6 February 2024; Revised: 11 March 2024; Accepted: 8 April 2024; Published: 15 April 2024

Abstract: Industrial development has accelerated soil contamination by organic pollutants, posing a major threat to global ecosystems and human health. Natural attenuation techniques, renowned for their environmental compatibility and cost-effectiveness, have garnered widespread attention for the remediation of environmental pollution. In this work, we have successfully enhanced the natural attenuation process of organic contaminants in soil by employing biostimulation and bioaugmentation methods to remove pollutants. The results showed that the degradation rate of low molecular weight polycyclic aromatic hydrocarbons (PAHs) reached about 82.5% while medium molecular weight PAHs was about 43.72%, as well as high molecular weight PAHs was about 34.5% even after a remediation process of only 14 days. In addition, the biofortified soil was exhaustively analyzed by high-throughput sequencing, which showed that the dosing of bactericide and surfactants significantly increased the abundance of 16sRNA genes and alkane degradation-related genes. In response to the challenges of detecting and analyzing complex organic pollutants in soil, we have developed an integrated method for the extraction, purification, and detection of organic pollutants in soil, ranging from low to medium concentrations. This approach not only allows for the efficient extraction of organic pollutants from the soil but also facilitates further inference of the degradation mechanisms of these pollutants. Integrating chemical analysis and microbiological techniques, and employing Gas Chromatography-Mass Spectrometry (GC-MS) and High-Resolution Mass Spectrometry (HRMS), we precisely measured and identified organic contaminants in soil and deduced the mechanisms of degradation. These findings are significant for the development of new environmental remediation technologies and strategies, contributing to addressing soil pollution issues exacerbated by industrial activities.

Keywords: polycyclic aromatic hydrocarbons (PAHs); total petroleum hydrocarbons (TPHs); low to moderate concentration; soil remediation; degradation mechanism

1. Introduction

With the rapid advance of global industrialization, the widespread use of diesel and other chemicals has led to the widespread distribution of organic pollutants in the ecosystem [1,2]. In particular, organic compounds such as polycyclic aromatic hydrocarbons (PAHs), total petroleum hydrocarbons (TPHs), and chlorinated hydrocarbons have become widespread representative substances in soil pollution [3]. These toxic substances can be transmitted through the food chain from prey to predator, and their unique physical and chemical properties allow them to persist in the environment for long periods and spread from the point of release to distant locations [4]. Long-term exposure to these compounds poses a significant risk to humans, with possible neurological damage to the respiratory, circulatory, liver, and kidneys [5,6]. Over the past few decades, we have witnessed tremendous progress in the field of environmental remediation, including the development of a wide range of physical remediation, bioremediation, chemical remediation [3], and Non-thermal plasma technology to deal with organic contaminants in soils [7,8]. However, many of the traditional physicochemical methods are

too expensive, compromise soil nutrient values, and can also lead to secondary contamination and the generation of hazardous waste, hence the need to find more effective remediation methods.

Natural attenuation is an environmental remediation method that has attracted much attention in recent years [9,10]. It is an intrinsic remediation process that degrades pollutants by stimulating native microorganisms in soil. Under normal circumstances, the degradation of pollutants by indigenous microorganisms in contaminated sites is a long process. Still, the metabolic capacity of degrading bacteria can be increased by strengthening natural attenuation, to improve the repair efficiency of contaminated sites. Enhanced natural attenuation can be achieved by using biostimulation and bioaugmentation strategies [11,12]. Biostimulation strategies entail the stimulation of native microbial activity within contaminated soil through the introduction of nutrients, electron acceptors, or surfactants [13,14]. This approach is especially well-suited for soils characterized by low nutrient levels and a substantial presence of petroleum hydrocarbons. This includes adjusting the C/N/P ratio in the soil to be closer to the ratio required by microorganisms, thereby increasing microbial activity, promoting the degradation of organic pollutants, and rapidly initiating the soil remediation process [15]. Bioaugmentation strategies, on the other hand, involve the introduction of specific microbial degraders and are particularly suitable for situations where local microbial populations are relatively small. These foreign microorganisms, such as Pseudomonas, Mycobacterium, Rhodococcus, and Sphingobacteria, not only stimulate the growth of native microorganisms but also directly promote the bioremediation process. These two strategies can be selected according to the characteristics of the soil and the number of microorganisms, which can help effectively reduce the soil pollution problem and restore the health of the soil ecosystem.

However, in cases involving complex mixtures of organic pollutants such as crude oil and PAHs, the degradation process becomes intricate and laborious. The hydrophobic and adsorptive properties of these pollutants make it challenging for microorganisms to establish contact with them. To overcome this issue, surfactants are introduced into the bioremediation process to enhance microbial accessibility to hydrocarbon compounds [16,17]. Surfactants can activate biodegradation through two distinct mechanisms: a) effectively dissolve organic compounds, allowing them to separate from soil particles and increasing the chances of microbial interaction with contaminants; b) Surfactants can change the surface properties of microbial cells and enhance their affinity for hydrophobic contaminants. For instance, the addition of non-ionic surfactants like Tween80, TritonX-100, and Brij30 can influence the surface characteristics of bacteria such as Pseudomonas GY2B, particularly in terms of membrane permeability, functional groups, and elemental composition [18]. Despite numerous laboratory studies verifying the efficacy of surfactants in the biodegradation of hydrocarbon compounds, there remains a scarcity of field research on this matter. Here, we amalgamate surfactants with exogenous microbial preparations to conduct in-situ remediation of organic-contaminated sites. The process of assessing the contamination status of an organically contaminated site typically involves the steps of extraction, purification, concentration, and detection. The traditional Soxhlet extraction method has become the standard method for extracting organic contaminants from complex environmental matrices [19–22]. However, this method suffers from several drawbacks, such as long extraction time, excessive amount of extractant, no stirring to accelerate the reaction, and tendency to lead to thermal degradation of analytes. In recent years, there have been significant advances in extraction techniques for organic contaminants in soil media, including ultrasonic extraction [23–26], solid-phase microextraction (SPME) [27,28], mechanical oscillation extraction [29,30], pressurized liquid extraction (PLE) [31], accelerated solvent extraction (ASE) [32,33], and microwave-assisted extraction (MAE) methods [34–36]. For example, ultrasonic extraction utilizes the force of fluctuations to efficiently extract analytes into the solvent, which reduces the consumption of organic solvents and improves efficiency [37]. In addition, the microwave-assisted extraction method heats the sample-solvent mixture with microwave energy, which induces the migration of the target substance from the sample matrix into the solvent and is characterized by high efficiency [35]. In addition, in the extraction process of soil organic pollutants, the selection of suitable extractants is a key factor to ensure the reliability and accuracy of the extraction results. Some commonly used extractants include n-hexane, dichloromethane, and acetone, which have different polar characteristics and applicable ranges. Among them, n-hexane, as a non-polar solvent, is widely used for the extraction of fat-soluble organic pollutants; dichloromethane's medium polarity makes it ideal for the extraction of pollutants with a wide range of applicability; and acetone, a polar solvent, can be used for the extraction of polar organics. However, the extraction rate can be affected by a variety of factors, including the type of extractant, liquid-solid ratio, extraction temperature, and extraction time. Response surface methodology (RSM) is an important technique in soil extraction optimization, aiming at determining the optimal levels of several parameters related to the extraction process and its effects [38–40]. The experimental design of RSM gives better results with less cost of testing and time compared to traditional experimental research methods. RSM

allows us to predict unmeasured data during the data analysis phase to obtain the best solution for the soil extraction process [41].

In this study, we have developed a method for the extraction, purification, and detection of organic pollutants designed to assess soil contamination and remediation status. Our research is centered on soil contamination predominantly caused by organic pollutants, employing biostimulation and bioaugmentation techniques to facilitate the natural degradation of organic contaminants in soil. As part of our bioremediation strategy, surfactants are introduced to enhance the bioavailability of pollutants, with changes in microbial community structure monitored to investigate the metabolic mechanisms of pollutant breakdown. Our approach integrates chemical analysis and microbiological techniques, utilizing Gas Chromatography-Mass Spectrometry (GC-MS), High-Resolution Mass Spectrometry (HRMS), and high-throughput sequencing to accurately measure and identify organic pollutants in soil. This study offers a novel perspective and methodology for addressing organic soil contamination through the synergy of chemistry and microbiology. By gaining a comprehensive understanding of the chemical properties of pollutants, their bioavailability, and the microbial community's response to contaminants, we are able to develop more effective soil remediation strategies aimed at minimizing environmental impact and providing cleaner soil for the future.

2. Methods and Materials

2.1. Chemicals and Instrumentation

Acetone (C_3H_6O, 99%), n-Hexane (C_6H_{14}, 99%), dichloromethane (CH_2Cl_2, 99.9%), Sodium sulfate anhydrous (Na_2SO_4, 99%), Potassium nitrate (KNO_3), Urea (H_2NCONH_2, 99.5%), Aminoacetic acid (NH_2CH_2COOH, 99%), Potassium dihydrogen phosphate (KH_2PO_4, 99.5%), Naphthalene ($C_{10}H_8$, 98%), Methanol (CH_3OH, 99.9%), Petroleum ether ($C_5H_{12}O_2$, bp 60–90 °C), Saponin ($C_{58}H_{94}O_{27}$) were provided by Aladdin Reagent Co., Ltd. D-(+)-Glucose ($C_6H_{12}O_6$, 99%), Phenanthrene ($C_{14}H_{10}$, 97%), Ammonium chloride (NH_4Cl), rhamnolipid, Humic acid, β-Cyclodextrin ($C_{42}H_{70}O_{35}$, 98%) were purchased from McLean Biochemical Technology Co., Ltd.

The instruments used in the experiment are analytical Balance (Gill International Trading (Shanghai) Co., Ltd.); Rotary evaporator (Shanghai Yarong Biochemical Instrument Factory); Oscillators (Shanghai Shiping Experimental Equipment Co., Ltd.); Microwave digestion apparatus (Gaohuan Youke (Shandong) Precision Instrument Co., Ltd.); Ultrasonic cell crusher (Shanghai Hushan Industrial Co., Ltd.); Freeze dryer (Changsha Bayue Instrument Co., Ltd.); Centrifuge (Shanghai Anting Scientific Instrument Factory); Uv-vis spectrophotometer (Platinum Elmer China); Ultra performance liquid chromatography (Shimadzu Company, Japan); Gas Chromatography-Mass Spectrometer (QP2020); Gas Chromatograph (GC-2030); Ultrasonic cleaner (Kunshan Ultrasonic Instrument Co., Ltd.); High-Resolution Mass Spectrometry (Thermo Scientific Q Exactive Focus).

2.2. Soil Sources and Storage

2.2.1. TPHs and PAHs Contaminated Soil Collection

Soils contaminated with low and medium concentrations of polycyclic aromatic hydrocarbons (PAHs) and petroleum hydrocarbons were sampled in Gongshu District, Hangzhou, at a sampling point located 200 cm below ground. The obtained soil samples were stored under seal at 4 °C and transported to the laboratory. The contaminated soil was removed from plant tissues, debris, and other foreign materials, mixed thoroughly, freeze-dried at −60 °C for 4 h to remove water, and the freeze-dried soil was ground and sieved with 200 mesh and stored at low temperature.

2.2.2. Preparation of Chlorinated Hydrocarbon Contaminated Soil

The subsoil in the garden was sampled using a soil sampler through drilling. The collected soil samples were spread evenly into a thin layer of 2–3 cm and placed in a ventilated cabinet, allowing them to air dry naturally at room temperature. Impurities such as plant roots, stems, and gravel were removed from the soil. After the soil had completely dried, it was finely ground using a ceramic mortar and pestle and passed through a 200-mesh sieve for thorough homogenization. A quantity of 1000 g of soil was weighed and mixed with 5 milligrams of trichloroethylene, creating a contaminated soil sample with a target concentration of 5 mg/kg. Contaminated soil samples were placed in sealed bags to prevent volatilization of contaminants and stored in a

dry, cool, and dark environment. They were left undisturbed for a period of 30 days to undergo aging under these conditions.

2.3. Enhanced Natural Attenuation

We investigated the impact of four different nitrogen sources, including organic nitrogen sources (urea and glycine) and inorganic nitrogen sources (potassium nitrate and ammonium chloride), on the performance of a bio-stimulant. Additionally, we examined the effects of varying soil carbon- nitrogen-phosphorus ratios, different soil moisture levels (10%, 30%, 50%), and different lighting conditions (darkness, natural light, >420 nm light) on the performance of the bio-stimulant. These experiments were conducted through various grouped batch trials, and specific experimental designs and results are documented in Table 1. By introducing microbial agents and enzyme formulations into organically polluted soil, we conducted a biostimulation approach. Additionally, we conducted combined biostimulation-bioaugmentation experiments by incorporating surfactants. The specific experimental design is detailed in Table 2.

Table 1. Biostimulation experimental design.

Treatment	Setup Composition
CK	Organic contaminated soil
B1	Organic contaminated soil + White rot fungus solid agent
B2	Organic contaminated soil + White rot fungus solid agent + Surfactant

Table 2. Bioaugmentation, biostimulation-reinforcement combined repair experimental design.

Treatment	Setup Composition
N1	Soil + C/N(NH_4Cl)/P (100/10/1) + 30% moisture content
N2	Soil + C/N(KNO_3)/P (100/10/1) + 30% moisture content
N3	Soil + C/N($CO(NH_2)_2$)/P (100/10/1) + 30% moisture content
N4	Soil + C/N($C_2H_5NO_2$)/P (100/10/1) + 30% moisture content
P1	Soil + C/N(NH_4Cl)/P (100/20/1) + 30% moisture content
P2	Soil + C/N(NH_4Cl)/P (100/30/1) + 30% moisture content
P3	Soil + C/N(NH_4Cl)/P (100/50/1) + 30% moisture content
M1	Soil + C/N(NH_4Cl)/P (100/10/1) + 10% moisture content
M2	Soil + C/N(NH_4Cl)/P (100/10/1) + 50% moisture content
L1	Soil + C/N(NH_4Cl)/P (100/10/1) + sunlight ($\lambda > 420$ nm)
L2	Soil + C/N(NH_4Cl)/P (100/10/1) + blackout treatment

2.4. Extraction Method Establishment

A single-factor experimental design was employed to establish an extraction method for PAHs and TPH in organically polluted soil by varying solvent type, extraction agent ratio, extraction time, and extraction method. Response surface methodology (RSM) was used to optimize the process conditions for ultrasound-assisted extraction, microwave-assisted extraction, shaking extraction, and ultrasonic cell disruption extraction. The extraction yield was selected as the response variable, and four independent variables, namely liquid-to-solid ratio (A), extraction time (B), extraction cycles (C), and extraction temperature (D), were investigated at three levels to develop a method for TCE extraction from soil. Design-Expert 8.0 software was employed to analyze 29 different experimental combinations. The selection of factors and their levels can be found in Tables S1 and S2. The specific steps of the extraction and purification method are described in Supplementary Materials Section S1.

2.5. Sample Analysis

Total petroleum hydrocarbon: The extracts were measured by gas chromatography with an initial temperature of 40 ℃, maintained for 1 min, and then ramped up to 340 ℃ at a rate of 30 ℃/min. The chromatographic column had a carrier gas flow rate of 2.89 mL/min, the injection method was split, and the detector temperature was 350 ℃.

Polycyclic aromatic hydrocarbons**:** The test liquid underwent analysis using a gas chromatography-mass spectrometry (GC-MS) instrument. Initially, the temperature was established at 60 °C and held steady for 1 min. Subsequently, a temperature ramp of 15 °C/min elevated it to 250 °C, where it remained for 0 min. Further temperature elevation at a rate of 5 °C/min ensued, reaching 310 °C and maintaining this temperature for 6 min.

The carrier gas flowed through the chromatographic column at a velocity of 1.50 mL/min. The injection method employed was the spitless mode, while the ion source and quadrupole temperatures were set at 230 °C and 150 °C, respectively. The scanning mode was configured as Scan, encompassing a mass scanning range spanning from 50.00 to 500.00 *m*/*z*.

Chlorinated hydrocarbons: The extracts were combined into a colorimetric tube, fixed to 10 mL with the extractant, and the resulting solution was measured for absorbance at 205 nm using an ultraviolet spectrophotometer.

2.6. DNA Extraction and Analysis of Microbial Community

The detailed experimental procedures are shown in the Supplementary Materials Section S2.

2.7. Theoretical Calculation Method

To gain deeper insights into the mechanism of alkane degradation, we employ Fukui indices based on density functional theory (DFT) to predict the regions in the molecule susceptible to attack. Utilizing Gaussian 16 software and the Gaussian View 6.0 interface, we have chosen the B3LYP functional and the 6–31 + G(d, p) basis set for geometry optimization and single-point energy calculations. By optimizing the geometric structure of the alkane molecule and computing single-point energies, we can accurately describe its energy minima and further calculate Fukui indices to identify potentially vulnerable atomic positions. This work contributes to unraveling the intricate mechanisms of alkane degradation, offering theoretical support for the development of more effective degradation methods.

3. Results and Discussion

3.1. Extraction Method Establishment

The extraction solvent has a significant influence on the extraction of organic pollutants. The extraction was optimized by changing different solvent combinations, and the results are shown in Figure 1a. The chromatographic and mass spectrograms were shown in Figure S1. 16 kinds of PAHs were extracted, 13 of which were best extracted with dichloromethane/acetone (1/1) as solvent. Acetone/n-hexane (1/1) has the best extraction effect on acenaphthene and benzo (a) anthracene, while n-hexane/dichloromethane (1/1) has the best extraction effect on benzo (k) fluoranthene. The extraction effect of the three extractants on total PAHs was dichloromethane/acetone (1/1) > acetone/n-hexane (1/1) > n-hexane/dichloromethane (1/1), which was related to the dielectric constant of the solvent (ε acetone = 20.7 > ε dichloromethane = 8.93 > εhexane = 1.88) [42]. This may be due to the fact that PAHs are hydrophobic, while acetone, as a polar solvent, has excellent solubility. In addition, dichloromethane also has a strong ability to dissolve. Therefore, in the solvent mixture of dichloromethane and acetone, there is a synergistic effect between the two, which enhances each other and improves the extraction efficiency. Furthermore, the extraction efficiency was evaluated by altering the ratio of dichloromethane and acetone to 3/7 and 7/3, as shown in Figure 1b. The experimental results showed that the extraction of soil PAHs using dichloromethane/acetone (1/1) solvent achieved the optimal extraction results even though the ratio of the extractant was changed. Generally, dichloromethane exhibits higher hydrophobicity, while acetone possesses higher polarity. Therefore, the dichloromethane/acetone (1/1) solvent mixture maintains a favorable balance between hydrophobicity and polarity, making it more suitable for the extraction process of PAHs. The properties and abbreviations of PAHs are shown in Table S9.

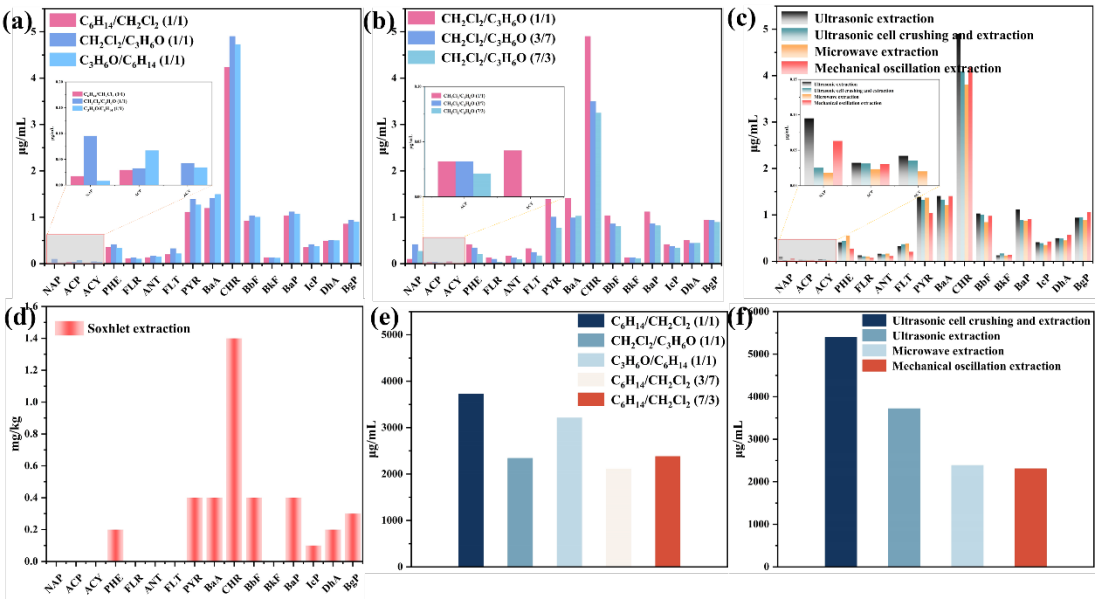

Figure 1. Extraction effect of soil contaminated with cycloaromatic hydrocarbons (**a**) different extractant combinations, (**b**) varying the ratio of different extractants, (**c**) varying different extraction methods, and (**d**) extraction effect of Soxhlet extraction. Extraction effect of soil contaminated with low and medium concentrations of petroleum hydrocarbons (**e**) different extractant combinations and varying the ratio of different extractants, (**f**) varying different extraction methods.

The most suitable extraction solvents were selected and several different extraction methods were tried to study PAHs in soil. These methods included ultrasonic extraction, mechanical oscillation extraction, microwave-assisted extraction, and ultrasonic cell breaker extraction. The results are shown in Figures 1c and S2, and the traditional ultrasonic extraction was the best for nine PAHs. This may be due to the fact that the high-frequency vibration property of ultrasound generates strong pressure waves and shear force in the liquid, which destroys the soil particle structure, increases the contact area between the solvent and PAHs, and improves the permeability and diffusion rate of the solvent, thus promoting the dissolution and extraction of PAHs [43,44]. For high molecular weight PAHs, the mechanical oscillation method has the best extraction efficiency. High molecular weight PAHs usually have larger molecular sizes and higher hydrophobicity, and therefore have a higher degree of solid-phase adsorption in soil, making it difficult to release and dissolve them quickly [45]. The mechanical oscillation method can provide strong mechanical shear force in a short period of time [46,47], which helps to overcome the limitations of solid-phase adsorption and mass transfer of high-molecular-weight PAHs, thus improving the extraction efficiency. In addition, according to the extraction results shown in Figure 1d, the Soxhlet extraction method failed to detect seven PAHs at low concentrations, including naphthalene, acenaphthene, acenaphthylene, fluorene, anthracene, fluoranthene, and benzo[k]fluoranthene. In contrast, the conventional ultrasonic extraction method was effective in releasing these compounds from the soil with a high detection range and sensitivity, providing a more comprehensive coverage of the various PAHs components in the soil.

Different extraction solvents were employed to extract total petroleum hydrocarbons from soil samples with medium to low concentrations of organic pollutants. The results, as shown in Figures 1e and S3, indicated that the extraction efficiency was optimized using a mixture of n-hexane and dichloromethane in a 1:1 ratio. The extraction efficiency of this solvent system was higher than that of a mixture of dichloromethane and acetone (1:1) by 58.97% and a mixture of acetone and n-hexane (1:1) by 15.89%. This is due to the fact that n-hexane and methylene chloride are both non-polar solvents that are very similar in chemistry and polarity. This similarity makes it easier for them to mix together to form a similarly phase-soluble mixture. It is easier to interact with non-polar substances (such as some petroleum hydrocarbon components), thus improving extraction.

The optimal extraction solvent (n-hexane/dichloromethane, 1/1) was used to extract total petroleum hydrocarbons from soil samples, employing different extraction methods including ultrasound-assisted extraction, sonication using an ultrasonic cell disruptor, microwave-assisted extraction, and mechanical agitation. The obtained results showed the maximum extraction efficiency of the ultrasonic cell disruptor as

shown in Figure 1f. This can be attributed to the generation of microbubbles through high-frequency sound wave vibrations produced by the ultrasonic cell disruptor [48]. These microbubbles induce intense eddy currents and physical impacts within the soil sample, effectively disrupting the adhesion between soil particles and petroleum hydrocarbons [49]. Consequently, the release and dissolution of petroleum hydrocarbons are facilitated. Additionally, the ultrasonic cell disruptor's high frequency and energy enable a faster extraction process, significantly reducing the chances of degradation or losses and thereby improving the extraction efficiency. The Soxhlet extraction method, which utilizes temperature to evaporate the target compounds from the sample and transfer them to the gas phase [50], was used for the extraction of total petroleum hydrocarbons from the soil with the poorest extraction efficiency compared to the other methods, as shown in Figures 1f and S4. This is mainly due to the narrow range of applicability of the Soxhlet extraction method, which may result in suboptimal extraction efficiency for specific compounds, especially those with high boiling points [51].

In order to extract and detect trichloroethylene in soil, Response Surface Methodology (RSM) was employed to optimize the process conditions for ultrasound-assisted extraction, microwave-assisted extraction, oscillatory extraction, and ultrasonic cell disruption. The response variable chosen was the extraction yield, and four independent variables, namely liquid-to-solid ratio (A), extraction time (B), number of extractions (C), and extraction temperature (D), were investigated at three levels. Based on the analysis of the response surface plots, microwave extraction exhibited the most favorable performance. The final determined optimal extraction conditions were as follows: liquid-to-solid ratio of 2.08 mL/g, extraction time of 13.93 min, three extraction cycles, and an extraction temperature of 50.03 degrees Celsius. According to the model predictions, the extraction yield reached 89.51%, as shown in Table 3. For a more detailed analysis process, please refer to Supplementary Materials Section S3.

Table 3. TCE extraction optimization results.

Extraction Method	Optimal Solution After Response Surface Optimization				Predicted Extraction Rate (%)
	A	B	C	D	
Ultrasonic extraction	1.77	14.32	3	60.00	84.49
Microwave Extraction	2.08	13.93	3	50.03	89.51
Mechanical oscillation extraction	2.91	15.30	3	35.26	72.20
Ultrasonic Cell Breaking and Extraction	Optimal extraction rate 72.03%				

A: Liquid-solid ratio; B: Extraction time; C: Extraction times; D: Extraction temperature.

In summary, we have established extraction, purification, and detection methods for three types of pollutants in typical organic-contaminated soils with medium to low concentrations. For the extraction of polycyclic aromatic hydrocarbons, we employed a solvent mixture of dichloromethane and acetone (1/1 ratio) and utilized the ultrasonic method. The extraction of petroleum hydrocarbons was conducted using an ultrasonic cell disruptor, with the optimal solvent being a mixture of dichloromethane and acetone (1/1 ratio). For the extraction of trichloroethylene, we employed a microwave extraction method with a solvent mixture of acetone and n-hexane (1/1 ratio), and we anticipate achieving an extraction efficiency of up to 89.51%.

3.2. Biostimulation

Biostimulation is considered a key factor in the enhanced natural attenuation of organic soil pollutants. Nitrogen is one of the key nutrients in bioremediation projects and is used to adjust the carbon-to-nitrogen ratio in the soil. It plays an important role in cell growth and as an electron acceptor, and is often added to soil in a variety of forms, such as urea, ammonium chloride, or other ammonium salts, all of which are easily absorbed by bacterial metabolism. We enhanced the natural attenuation of organic pollutants in the soil by adding different nitrogen sources, changing the soil carbon, nitrogen, and phosphorus ratios, and altering water content and light conditions. The experimental results are shown in Table 4. For most pollutants (NAP, ACP, ACY, PHE, FLR, ANT, PYR, BkF, BaP, IcP, BgP), NH_4Cl appears to be a favorable nitrogen source (Figure 2). Ammonium chloride, as a nitrogen source, is easily absorbed and utilized by microorganisms and has been shown to stimulate the activity of microorganisms involved in the degradation of PAHs [52]. For total petroleum hydrocarbons, on the other hand, glycine was selected as the optimal nitrogen source (Figure S14a). Maintaining an appropriate carbon/nitrogen/phosphorus ratio is essential to facilitate the degradation of PAHs and TPHs.

Figures S9 and S14b show the changes of 16 PAHs in soil under different C/N/P ratios. After changing the C/N/P ratio of soil, the PAHs content showed a decreasing trend in all cases. Especially when the soil C/N/P ratio is 100/30/1, the declining trend is most obvious, indicating that this ratio is most conducive to the natural degradation of PAHs and TPHs. Excessive addition of nitrogen may inhibit biodegradation, as excess ammonia has a toxic effect on the growth of soil microorganisms [53].

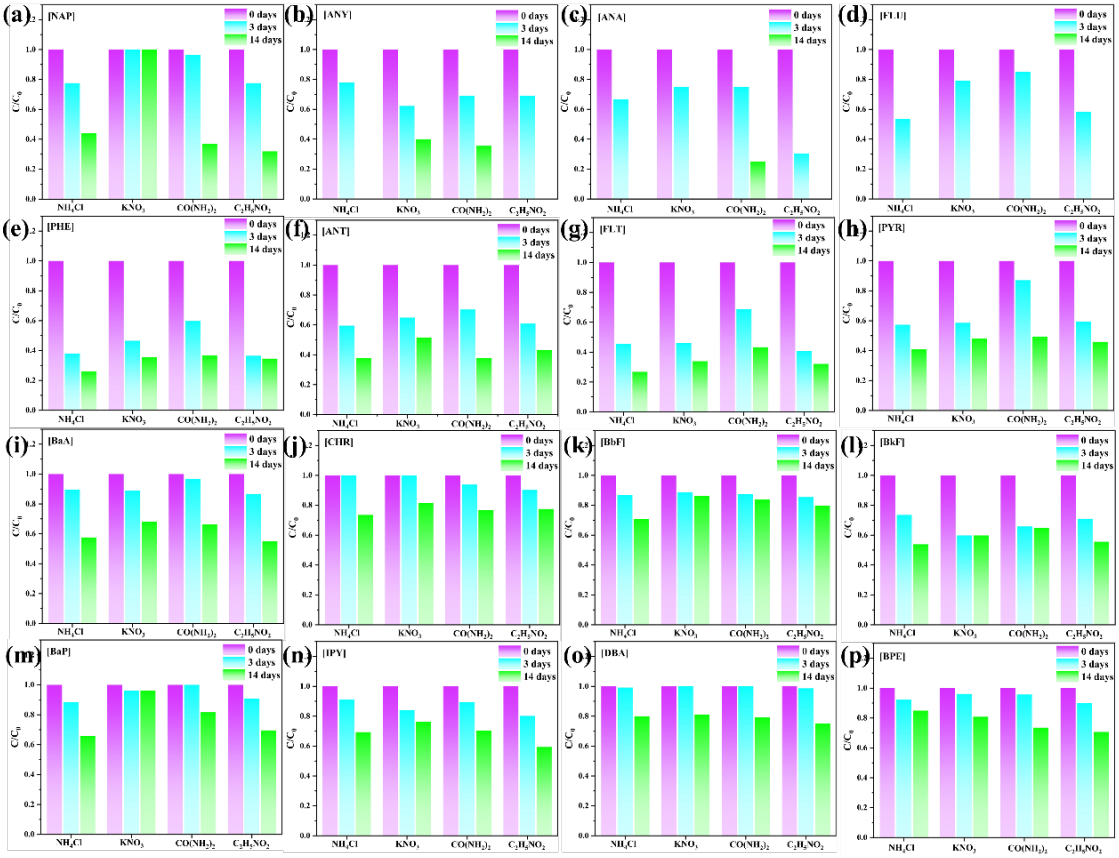

Figure 2. Effect of different nitrogen sources (NH_4Cl, KNO_3, $CO(NH_2)_2$, $C_2H_5NO_2$) on the natural attenuation degradation of 16 PAHs, a-p for NAP, ANY, ANA, FLU, PJE, ANT, FLT, PYR, BaA, CHR, BbF, BkF, BaP, IPY, DBA, BPE.

Table 4. Results of biostimulation for remediation of organically contaminated soil.

	Optimal Nitrogen Source				Optimal Carbon, Nitrogen, and Phosphorus Ratio				Optimum Moisture Content			Optimal Light Conditions		
	NH_4Cl	**KNO_3**	**$CO(NH_2)_2$**	**$C_2H_5NO_2$**	**100/10/1**	**100/20/1**	**100/30/1**	**100/50/1**	**10%**	**30%**	**50%**	**Natural Light**	**Light > 420 nm**	**Shade**
NAP	★	-	-	-	-	★	-	-	★	-	-	-	★	-
ACP	★	-	-	-	-	-	★	-	-	★	-	★	-	-
ACY	★	-	-	-	-	-	★	-	-	★	-	-	★	-
PHE	★	-	-	-	-	-	★	-	-	★	-	★	-	-
FLR	★	-	-	-	-	-	★	-	-	★	-	★	-	-
ANT	★	-	-	-	-	-	★	-	-	★	-	★	-	-
FLT	★	-	-	-	★	-	-	-	-	★	-	★	-	-
PYR	★	-	-	-	-	-	★	-	-	★	-	★	-	-
BaA	-	-	-	★	-	-	★	-	-	-	★	★	-	-
CHR	★	-	-	-	-	-	★	-	-	-	★	★	-	-
BbF	★	-	-	-	★	-	-	-	-	★	-	★	-	-
BkF	★	-	-	-	-	-	★	-	-	-	★	★	-	-
BaP	★	-	-	-	★	-	-	-	-	★	-	★	-	-
IcP	-	-	-	★	-	-	★	-	-	-	★	-	★	-
DhA	-	-	-	★	-	-	★	-	★	-	-	-	★	-
BgP	-	-	-	★	-	-	★	-	★	-	-	-	-	★
TPHs	★	-	-	-	-	★	-	-	-	-	★	★	-	-

Water content is an important factor affecting soil conditions, so we investigated the influence of different soil water content on the bioremediation process of PAHs contaminated soil. After 14 days of remediation, it was found that maintaining a soil water content of 30% was most favorable for the attenuation of most PAHs (Figure S10). Total petroleum hydrocarbons, on the other hand, require a somewhat higher water content to achieve 60% degradation, as shown in Figure S14c. In addition, we investigated three different light conditions, and the experimental results are shown in Figures S11 and S14d. Most of the pollutants showed the best degradation under natural light conditions (ACP, ACY, PHE, FLR, ANT, FLT, PYR, BbF, BaP, TPHs), indicating that regular daylight was conducive to microbial activity and pollutant degradation. Sunlight can also improve the soil microenvironment and enhance the metabolic activity of microorganisms.

After a 14-day natural attenuation study, we assessed the degradation of PAHs and categorized them based on their molecular weight into low, medium, and high molecular weight groups (LMW, MMW, HMW). The results show that the average degradation rate of low molecular weight PAHs (including naphthalene to anthracene) is approximately 82.5%, medium molecular weight PAHs (including phenanthrene to chrysene) have a degradation rate of approximately 43.72%, while high molecular weight PAHs (including benzo(b)fluoranthene to benzo(g,h,i)perylene) have a degradation rate of approximately 34.5%. As the molecular weight increases, the degradation rate gradually decreases, which may be due to the complex molecular structure of high molecular weight PAHs posing challenges for microbial degradation. Furthermore, through the above experiments, we have validated the wide applicability of our developed method for the extraction, purification, and detection of PAHs and TPHs in complex soils. This method can not only detect low to moderate concentrations of pollutants but can also accurately detect soil after natural attenuation, providing comprehensive test results. By comprehensively analyzing the experimental results, we have successfully identified the extreme conditions that influence the natural attenuation of different types of PAHs. These conditions include the selection of nitrogen sources, carbon-to-nitrogen ratios, moisture content, and light conditions, which are expected to significantly promote the in-situ biodegradation of PAHs and TPHs. This discovery provides a solid scientific basis for the remediation of environmental pollutants.

Surfactants have a critical role in the natural attenuation of organically contaminated soils. Surfactant addition may positively affect the reduction of surface tension and increase the solubility of contaminants through micellar solubilization, thus improving the bioavailability of contaminants. In this study, we used five different surfactants to enhance the effect of natural attenuation for naphthalene-contaminated garden soil, humus, and laterite. For garden soil and humus soil (Figure 3a,c), the addition of rhamnolipids resulted in naphthalene degradation of 82.9% and 87.5% within 14 days, respectively. In contrast, the addition of cyclodextrins showed the best natural attenuation in red soil, but the degradation rate was only 48.7% (Figure 3b). In addition, the natural attenuation effect on naphthalene varied according to different soil types, in the following order: humus soil > garden soil > laterite soil. This is mainly because humus soils are rich in organic matter and microbial communities, which provide nutrients and substrates that help promote the decomposition of PAHs. In contrast, lateritic soils have relatively low organic matter content, and therefore their ability to attenuate PAHs naturally is weak. The differences in the degradation effects of different surfactants can indeed be attributed to differences in their properties and structures. Cyclodextrin (CD), as a surfactant, can encase hydrophobic substances in the internal hydrophobic cavity to form water-soluble inclusion compounds, thus greatly improving the water solubility and water phase stability of hydrophobic small molecules. Promote the transfer of lipophilic to hydrophilic, improve water solubility, and thus increase the degradation rate [54]. As shown in Figure 3d, rhamnolipids are bioanionic surfactants produced by Pseudomonas aeruginosa, which are widely used to promote the biodegradation of hydrocarbons. The double rhamnose-lipids used in this study contain a hydrophilic head of an α-L-rhamnose-pyranose ring ($C_6H_{12}O_5$) and carboxylic group (-COOH), and a hydrophobic tail of a β-hydroxy acid. Studies have shown that rhamnolipids have the ability to promote the desorption of PAHs in soil [55], and can effectively dissolve organic matter and enhance biodegradation [56]. In addition, rhamnolipid can change the hydrophobicity of cells, change the interaction between microbial cells and naphthalene, and make cells more easily in contact with pollutants, which is conducive to the adsorption and growth of microbial cells, and cells with high hydrophobicity have a higher efficiency of degrading pollutants. Therefore, the attenuation of pollutants is strengthened under the dual action. From a toxicity perspective, rhamnolipids, as biosurfactants, are typically considered to have low toxicity in environmental contexts due to their complete biodegradability, which reduces the likelihood of accumulation and long-term pollution [57]. Additionally, rhamnolipids are characterized by their non-toxic and non-polluting properties, and they have shown promise in a variety of fields including medicine, food, and agriculture.

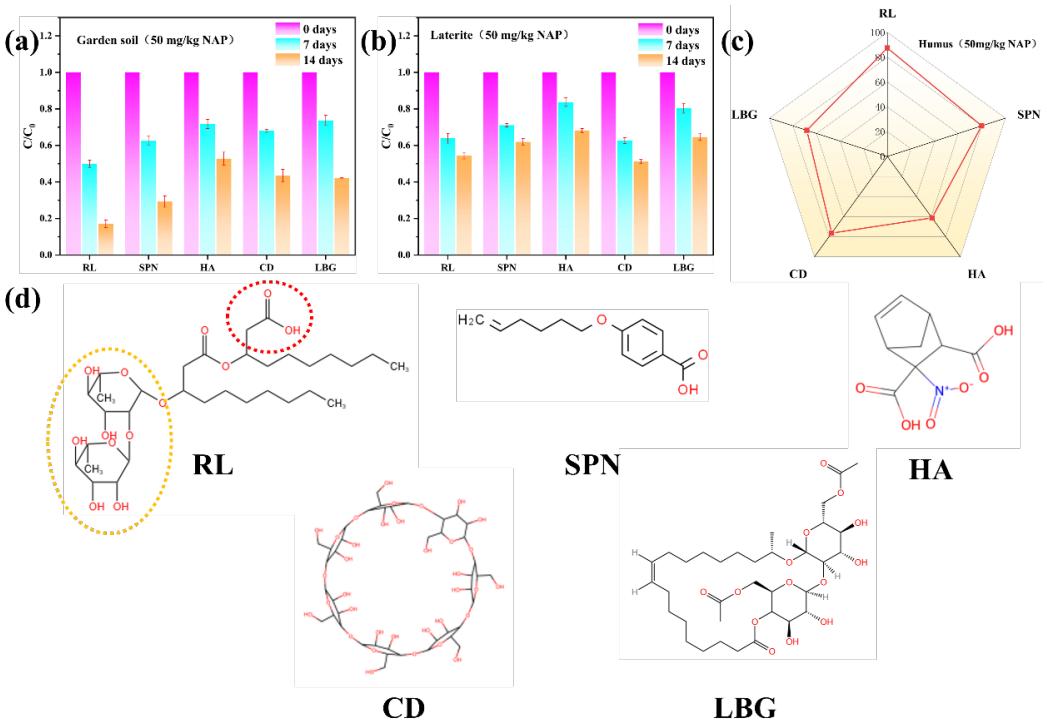

Figure 3. 50 mg/kg naphthalene contaminated soil natural attenuation experiment (**a**) Garden soil, (**b**) Laterite soil, (**c**) Humus soil, (**d**) Structure of RL, SPN, HA, CD, and LBG. In the figure, RL, SPN, HA, CD, and LBG denote the addition of Rhamnolipids, Saponin, Humic Acid, Cyclodextrin, and Locust Bean Gum.

3.3. Degradation Mechanism of Alkanes

3.3.1. Bacterial Community Diversity and Richness

Biostimulation and bioaugmentation have both been shown to improve the degradation efficiency of organic pollutants [58,59]. Previous studies have shown that the combined application of biostimulation and bioaugmentation can be more effective in enhancing the metabolic activity and biomass of microorganisms, thereby improving the degradation efficiency of contaminants. Two remediation methods were used to treat soil contaminated with a mixture of alkanes, and the soil was tested for 16 s after 60 days of remediation. The raw data obtained from sequencing (Raw Data), there is a certain amount of interference data (Dirty Data), in order to get high-quality sequencing data, to improve the accuracy of the subsequent bioinformatic analysis, firstly, we need to splice the raw downstream data, and then carry out the quality control and filtration, to get the valid data (Clean Data). The sequencing data volume and quality statistics of the samples are shown in Table S14. Sequences are clustered with a similarity of 97%; sequences with a similarity greater than 97% will be clustered into the same OTU, and the resulting OTU-representative sequences will be used for subsequent species annotation. The microbial richness and diversity of three soil samples were analyzed, as shown in Table 5, using four indexes: Shannon, Simpson, Chao1, and ACE. Chao1 and ACE are mainly used to evaluate species richness in samples [60]. As can be seen from the Chao1 and ACE indices, their order is B2 > B1 > CK, indicating that the species richness of the B2 sample is the highest, while the CK sample is the lowest. In cases where a combination of microbial and surfactants were used to repair and strengthen the natural decay of the mixed pollutants, microbial abundance reached its highest level within 60 days. In addition, according to the Simpson index, the order of species diversity is also B2 > B1 > CK, which means that B2 samples have the highest species diversity. It is speculated that B2 has a better effect on repairing organic polluted soil.

Table 5. Alpha Diversity Index Analysis.

Sample	Sobs	Chao1	ACE	Shannon	Simpson	Invsimpson	Coverage
CK	330	367.5	378.4907	1.085924	0.65336	1.53055	0.997745
B1	1544	1734.099	1829.483	4.025824	0.127537	7.840842	0.988951
B2	2402	3737.6	3651.667	4.891586	0.085112	11.7492	0.969936

3.3.2. Composition of Bacterial Communities

To explore the effects of biostimulation and bioenhancement on soil microbial communities, we studied the synergistic interaction between White rot fungus solid agent and surfactants to analyze their effects on the composition of soil bacterial communities. Using the original soil CK as a control group, we analyzed the soil of three different treatments at the phylum level (Figure 4a–c). In the control group, Proteobacteria was the dominant microbial phylum, occupying 97.35% of the relative abundance, while the other phylum occupied 2.65%. After dosing of White rot fungus solid agent, Proteobacteria remained dominant but the relative abundance decreased to 81.25% while the relative abundance of microbial phyla such as Actinobacteria (6.21%), Gemmatimonadetes (5.01%) and Bacteroidetes (2.39%) increased significantly. The relative abundance of Proteobacteria further decreased to 68.82% in the group with the addition of White rot fungus solid agent combined with surfactant. Meanwhile, the relative abundance of other microbial phyla increased significantly including Actinobacteria (14.27%), Gemmatimonadetes (7.38%), Bacteroidetes (2.89%), Deinococcus-Thermus (1.14%), Bacteria_unclassified (2.27%). These results indicate that the White rot fungus solid agent and synergistic application of White rot fungus solid agent and surfactants increased soil microbial diversity, especially the relative abundance of Actinobacteria, Gemmatimonadetes, and Bacteroidetes. Previous studies have also shown that Actinobacteria, Gemmatimonadetes, and Bacteroidetes have a strong ability to degrade organic pollutants [61].

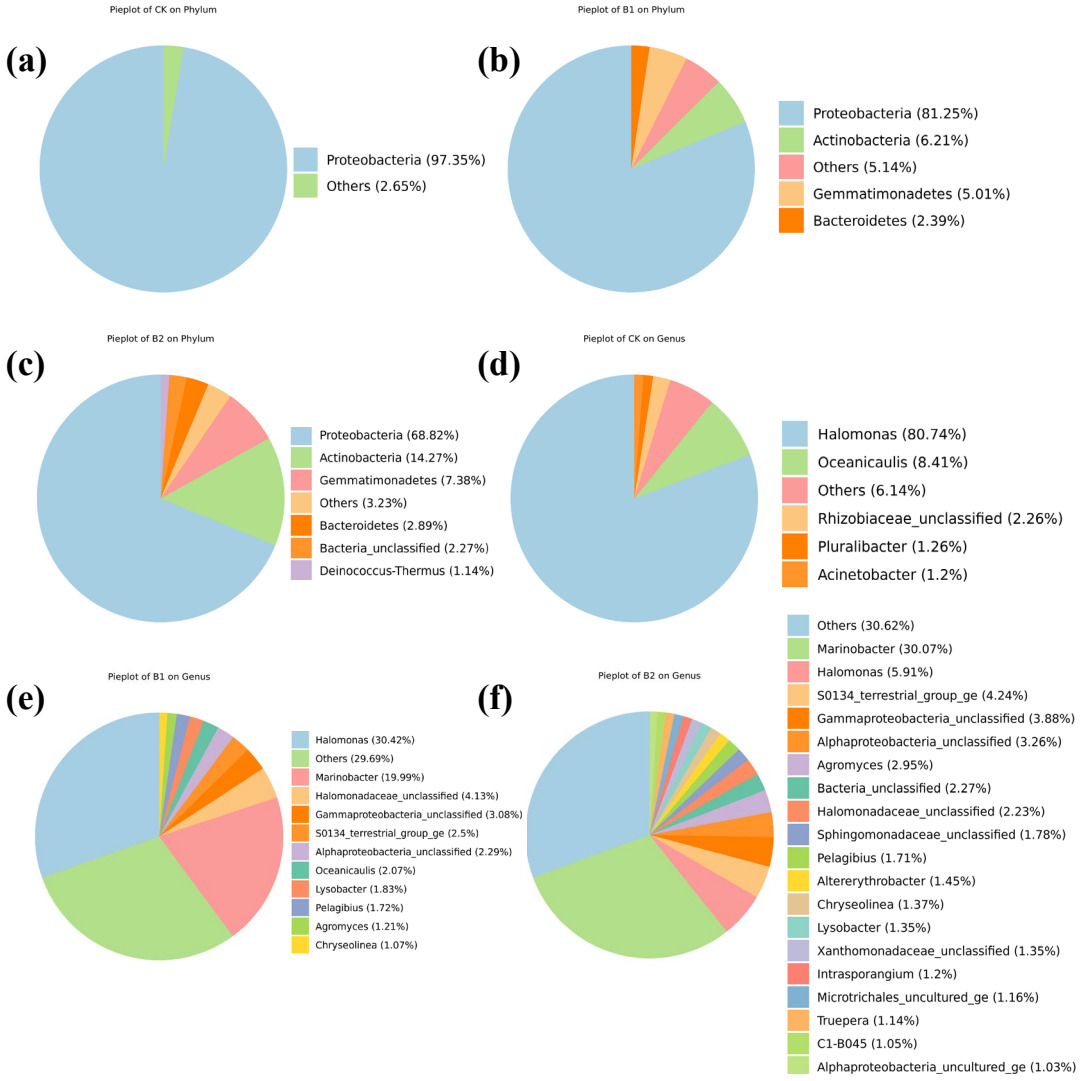

Figure 4. Soil microbial communities analyzed at the phylum (**a–c**) and genus (**d–f**) levels. CK: Control group, B1: microbiological agent, B2: Synergistic application of microbial treatments with surfactants.

At the genus level (Figure 4d–f), the predominant microbial genus of alkane-contaminated soil was Halomonas, which occupied 80.74% of the relative abundance, whereas other microbial genera had relatively

low relative abundance. The relative abundance of Halomonas (30.42%) decreased significantly after the application of the White rot fungus solid agent, while the relative abundance of Marinobacter (19.99%) and other microbial genera increased significantly. The relative abundance of Halomonas further decreased to 5.91% and Marinobacter (30.07%) became the dominant microbial genus after the dosing of bacteriophage combined with surfactant. The relative abundance of other microbial genera also increased significantly, including Agromyces, S0134_terrestrial_group_ge, and Gamma proteobacteria_ unclassified. These results suggest that the White rot fungus solid agent/White rot fungus solid agent and surface-activator treatments, which affected the soil microbial genus composition, resulted in a decrease in the relative abundance of Halomonas and an increase in other microbial genera. Studies have shown that increased Marinobacter increases the biodegradation of organic pollutants [62–64]. Figure 5a–c illustrate the changes in species composition at multiple levels. Compared to the CK treatment, the B1 and B2 treatments showed an increase in the number of species at multiple taxonomic levels, including kingdom, phylum, order, family, and genus. This suggests that the B1 and B2 treatments may be more conducive to enhancing the bioremediation effects of natural attenuation. Detailed information is provided in support materials Figures S15–S17. Kyoto Encyclopedia of Genes and Genomes was used to study the genome, metabolic pathways, and biological functions (Figure 5d). The analysis showed that B1/B2 treatment enhanced the abundance of microorganisms with degradation functions, such as Geraniol degradation, Caprolactam degradation, Limonene and pinene degradation, Aminobenzoate degradation, and Bisphenol degradation, etc., which may promote bioremediation of organic pollutants. Detailed information is provided in Tables S15 and S16.

In order to demonstrate the advantages and development prospects of white rot fungi solid bactericides combined with surfactants in the degradation of organic pollutants, the following table compares several different methods for the degradation of organic pollutants (Table 6). Each method has its own characteristics and scope of application, and the method of white rot fungus solid agent combined with surfactant may show better performance or have specific advantages under certain conditions.

Table 6. Environmental impacts of different methods for degrading organic pollutants.

Method	Advantages	Disadvantages	Environmental Impact	References
Chemical Oxidation Method	High degradation efficiency	Requires large amounts of chemical reagents, generating secondary pollution and higher costs	Medium to high	[65]
Photocatalytic Degradation	Environmentally friendly, no additional chemicals required	Requires a light source and is dependent on lighting conditions	Low	[66]
Adsorption Method	Simple operation and high efficiency	Inability to degrade contaminants, requiring periodic replacement of adsorbents	low to medium	[67]
White rot fungi combined with surfactant methods	Environmentally friendly, widely applicable, cost-effective	Degradation may be slow	Low	This study

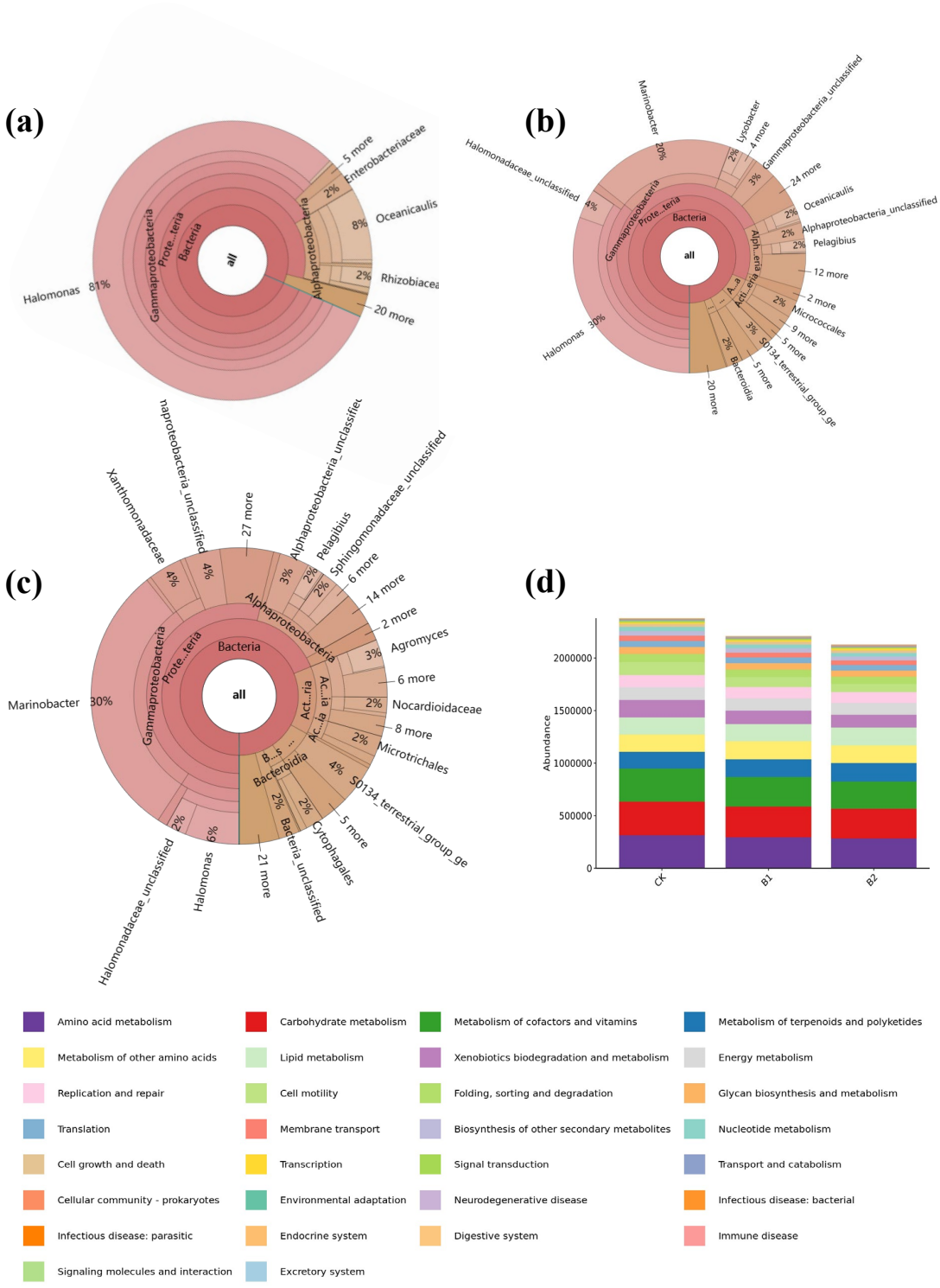

Figure 5. Multilevel species composition diagrams for (**a**) CK, (**b**) B1, and (**c**) B2, from the innermost circle to the outer circle, in order of species composition at the level of kingdom, phylum, order, family, and genus; (**d**) KEGG_pathway Stacked Bar Chart (level2).

3.3.3. Effect of Bacterial Composition on Biodegradation of Alkane-Contaminated Soil

Mixed alkane contaminated soil was bioremediated with microbial agents and surfactants, and GC-MS tests were performed on the 30th and 60th days of remediation. Due to the complexity of organic pollutant species in the soil, we analyzed compounds in the range of different carbon chain lengths. Significant trends were observed for different compounds during the remediation process (Tables S17–S21). In the C10–C20 range, the relative content of Hexadecane showed a slight decrease from the initial 0.84 to 0.69 on day 60. In

the C20-C30 range, special attention was paid to Heptadecane and Octadecane, where the relative content of Heptadecane was higher on day 0 but decreased significantly on day 60, while the content of Octadecane decreased from 0.87 to 0.69. In the C30–C50 range, the concentration of long carbon chains of undecane and tetradecane compounds showed a significant decreasing trend (Figure 6). By analyzing the soil microorganisms, we found that the alkane contaminants in the soil were undergoing natural degradation. This may be related to the changes in the soil microbial community after we injected microbial agents and surfactants. Also, the number of functional microorganisms with degradation ability in the soil increased, indicating the possibility of their decomposition during the remediation process.

Subsequently, we utilized High-Resolution Mass Spectrometry (HRMS) to explore the potential degradation pathways of tetracontane under environmental conditions enhanced with the addition of microbial agents and surfactants over a span of 30 days, as depicted in Figure S18. The MetabolitePilot software facilitated the identification of seven possible degradation products (Figure S18b–h), with their mass spectra juxtaposed against the baseline spectrum of the initial tetracontane. The molecular formulas of each product were annotated and differentiated by their respective *m*/*z* ratios. The original tetracontane displayed a prominent molecular ion peak (FigureS18a), which exhibited a notable reduction in intensity after 30 days, indicating that the molecule may have undergone processes such as photolytic or biotic degradation. This alteration was accompanied by an increase in the relative abundance of the seven potential degradation products (Figure S18b–h). Specifically, in Figure S18d and Figure S18h, we noted a significant rise in the peaks of smaller molecular ions, representing the cleavage of molecular chains and the generation of shorter chain fragments. The emergence of these degradation products shed light on the potential cleavage patterns of tetracontane, suggesting the relative stability of C-C and C-H bonds during the compound's degradation process. For example, the formation of $C_6H_{15}^+$ (Figure S18d) indicates the likelihood of α-cleavage or β-cleavage, while the appearance of $C_2H_3^+$ (Figure S18h) may suggest more intricate mechanisms of cleavage, such as internal hydrogen transfer or cyclization reactions.

In the study of the degradation process of tetracontane, theoretical calculations of Fukui indices drew our attention to the carbon atoms at positions C17, C18, C38, and C39. These positions exhibited higher local reactivity, indicating a higher likelihood of undergoing cleavage during chemical reactions (see Supplementary Materials Table S22). The prediction of these cleavage points is based on changes in electron density, reflecting the propensity of these carbon atoms to participate in electrophilic or nucleophilic attacks during chemical reactions. Coupled with high-resolution mass spectrometry analysis, we observed several ionic fragments, namely $C_5H_{13}^+$, $C_6H_{15}^+$, and $C_7H_{17}^+$ (Figure 7). The presence of these ionic fragments directly mirrors the specific chain-breaking mechanisms experienced during the molecule's degradation, aligning with the active cleavage points predicted by the Fukui indices, thereby reinforcing the reliability of theoretical calculations and their correlation with experimental outcomes. This data provides us with invaluable information regarding the environmental stability and degradation kinetics of tetracontane, which is imperative for environmental risk assessment and the development of pollutant management strategies.

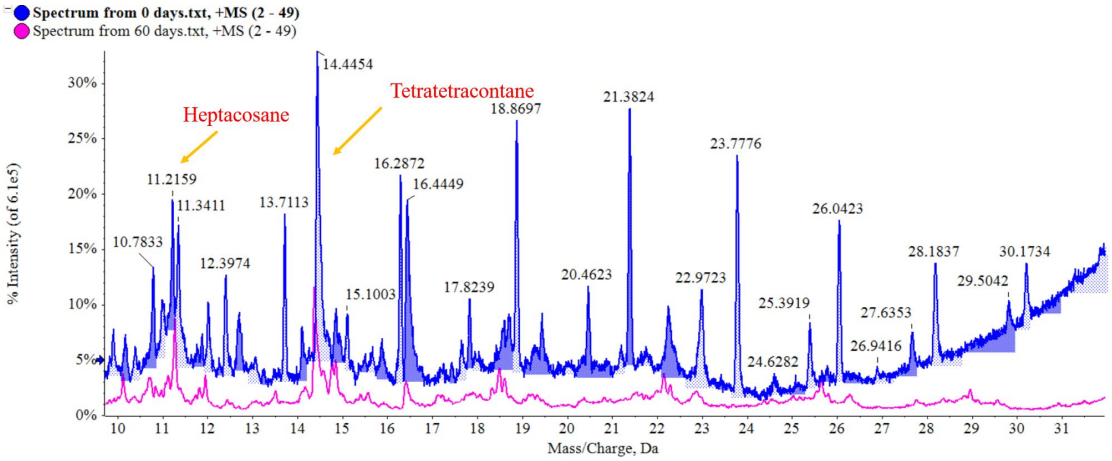

Figure 6. Gas chromatogram of soil contaminated with mixed alkanes.

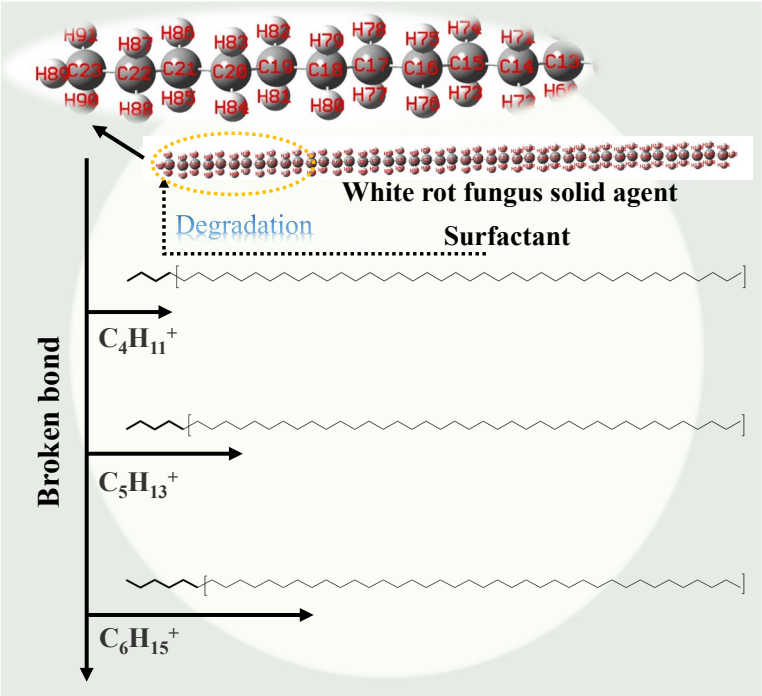

Figure 7. Degradation mechanism of tetradecane in soil.

4. Conclusions

In this study, we have examined the impact of bio-stimulation and bio-augmentation, individually and in synergy, on the natural degradation of organic pollutants within soil environments. We assessed the bio-stimulation of PAHs and TPHs by manipulating variables such as organic/inorganic nitrogen sources, soil C/N/P ratios, moisture content, and light exposure. Optimal degradation conditions were identified: using ammonium chloride as a nitrogen source, a C/N/P ratio of 100/30/1, and maintaining 30% soil moisture content under natural light conditions resulted in pronounced attenuation of PAHs and TPHs. A marked acceleration in the degradation process was observed under these conditions, with low molecular weight PAHs degrading by up to 82.5% within a 14-day period. Further, we explored the bio-remediation potential of five different surfactants on garden soil, humus soil, and lateritic soil. Remarkably, the addition of rhamnolipid to garden and humus soils achieved naphthalene degradation rates of 82.9% and 87.5%, respectively, within 14 days. Crucially, a novel remediation strategy was introduced that combines bio-stimulation and bio-augmentation. This approach, leveraging White rot fungus solid agent binding surfactant significantly reduced C30-C40 alkane concentrations in mixed pollutant-contaminated soils over a 60-day period. Post-remediation soil analysis, via 16S rRNA gene sequencing, revealed an increase in the soil microbial population, especially those microbes capable of degrading pollutants. Additionally, our methodology for extracting, purifying, and detecting low to medium concentration organic pollutants was affirmed, showing efficacy in treating complex soil matrices. HRMS enabled us to propose potential cleavage pathways during the degradation of $C_{44}H_{90}$. These findings are instrumental in providing scientifically grounded approaches for remediating sites contaminated with organic pollutants at varying concentrations.

Supplementary Materials: The following supporting information can be downloaded at: https://www.sciltp.com/journals/see/2024/1/334/226, Figure S1: Optimized Chromatograms and Mass Spectra of Polycyclic Aromatic Hydrocarbons (PAH) Extractants; Figure S2: Optimization of extraction methods for polycyclic aromatic hydrocarbons by chromatography and mass spectrometry; Figure S3: Optimized chromatograms of petroleum hydrocarbon extractants (a) dichloromethane/n-hexane (1/1), (b) dichloromethane/acetone (1/1), (c) n-hexane/acetone (1/1), (d) dichloromethane/n-hexane (7/3), (e) dichloromethane/n-hexane (3/7) ; Figure S4: Optimized chromatograms of petroleum hydrocarbon extraction methods (a) ultrasonic extraction, (b) microwave extraction, (c) mechanical oscillation extraction, (d) ultrasonic cell breaker extraction, and (e) soxhlet extraction; Figure S5: Standard curve (a) The extractant was n-hexane, (b) The extractant was n-hexane/acetone (1/1); Figure S6: Normal probability distribution of residual, residual and predicted value distribution, predicted and actual value distribution: ultrasonic extraction (a–c), microwave extraction (d–f), oscillation extraction (g–i); Figure S7: Response surface analysis of ultrasonic extraction (a–f), microwave extraction (g–l) and mechanical oscillation extraction (m–r); Figure S8: Extraction of TCE by ultrasonic cell crusher at different extraction times (2.5, 5.0, 7.5 min) and different ultrasound on/off times; Figure S9: Effect of varying soil carbon/nitrogen/phosphorus ratios (100/10/1, 100/20/1, 100/30/1, 100/50/1) on the degradation of 16 PAHs by natural

attenuation, a-p for NAP, ANY, ANA, FLU, PJE, ANT, FLT, PYR, BaA, CHR, BbF, BkF, BaP, IPY, DBA, BPE; Figure S10: Effect of varying soil moisture content (10%, 30%, 50%) on the natural attenuation degradation of 16 PAHs, a-p for NAP, ANY, ANA, FLU, PJE, ANT, FLT, PYR, BaA, CHR, BbF, BkF, BaP, IPY, DBA, BPE; Figure S11: Effect of varying light conditions (natural light, >420 nm, light-avoidance treatment) on the degradation of 16 PAHs by natural attenuation, a-p for NAP, ANY, ANA, FLU, PJE, ANT, FLT, PYR, BaA, CHR, BbF, BkF, BaP, IPY, DBA, BPE; Figure S12: PAHs natural attenuation remediation for 3 days, plots a-l in order L1, L2, M1, M2, N1, N2, N3, N4, P1, P2, P3, CK (logarithmic scale); Figure S13: PAHs natural attenuation restoration for 14 days, plots a-l in order N1, N2, N3, N4, P1, P2, P3, M1, M2, L1, L2; Figure S14: TPHs natural attenuation restoration for 14 days, (a) Addition of different nitrogen sources, (b) Changing soil carbon, nitrogen and phosphorus ratios, (c) Changing soil moisture content, (d) Varying light conditions; Figure S15: Multilevel species composition of the control group (CK); Figure S16: Multilevel species composition of the control group (B1); Figure S17: Multilevel species composition of the control group (B2); Figure S18: Degradation mechanism of tetradecane in soil; Table S1: Ultrasonic and Mechanical Oscillation Extraction Parameter Settings; Table S2: Microwave extraction parameter Settings; Table S3: Instruments and Reagents; Table S4: Default primers and standard experimental conditions; Table S5: Prepare the PCR reaction system; Table S6: Place the PCR tubes in the PCR machine and run the program; Table S7: Prepare the second round of the PCR reaction system; Table S8: Place the PCR tubes in the PCR machine and run the program; Table S9: Polycyclic aromatic hydrocarbon properties; Table S10: Experimental design of trichloroethane contaminated soil using ultrasonic extraction and extraction rates; Table S11: Experimental design of trichloroethane contaminated soil using mechanical oscillation extraction and extraction rates; Table S12: Experimental design of trichloroethane contaminated soil using microwave extraction and extraction rates; Table S13: ANOVA of quadratic model for ultrasonic extraction, microwave extraction, and mechanical oscillation extraction; Table S14: Sequencing data volume and quality statistics of samples; Table S15: KEGG_pathway detailed data (level3); Table S16: KEGG_pathway Specific hierarchical relationships (level 1–3); Table S17: GC-MS results for mixed alkane contaminated soil (0 days); Table S18: Mass spectra of GC-MS tests of mixed alkane contaminated soils (0 days) ; Table S19: GC-MS results for mixed alkane contaminated soil (30 days); Table S20: GC-MS results for mixed alkane contaminated soil (60 days); Table S21: Mass spectra of GC-MS tests of mixed alkane contaminated soils (60 days); Table S22: Fukui Index Analysis for tetradecane.

Author Contributions: Conceptualization, X.B., W.S. and L.G.; validation, W.S.; resources, X.B. and L.G.; data curation, W.S.; writing—original draft preparation, W.S.; writing—review and editing, X.B.; supervision, X.B., R.L., Y.C., P.J., B.Z. and X.Z. All authors have read and agreed to the published version of the manuscript.

Funding: This research was funded by National Key R&D Program of China (2020YFC1808805), National Natural Science Foundation of China (22276011, 21607034), Beijing Natural Science Foundation (8192011), Science and Technology General Project of Beijing Municipal Education Commission (KM202010016006), the Pyramid Talent Training Project of Beijing University of Civil Engineering and Architecture (JDYC20200313), the Cultivation project Funds for Beijing University of Civil Engineering and Architecture (X23042), the Outstanding Talent Project of Beijing Xicheng District (202323) .

Data Availability Statement: Not applicable.

Conflicts of Interest: The authors declare no conflict of interest.

References

1. Kwon, J.-H.; Ji, M.-K.; Kumar, R.; Islam, M.M.; Khan, M.A.; Park, Y.-K.; Yadav, K.K.; Vaziri, R.; Hwang, J.-H.; Lee, W.H.; et al. Recent advancement in enhanced soil flushing for remediation of petroleum hydrocarbon-contaminated soil: A state-of-the-art review. *Rev. Environ. Sci. Bio/Technol.* **2023**, *22*, 679–714. https://doi.org/10.1007/s11157-023-09657-0.
2. Wu, Z.; Chen, Y.; Yang, Z.; Liu, Y.; Zhu, Y.; Tong, Z.; An, R. Spatial distribution of lead concentration in peri-urban soil: Threshold and interaction effects of environmental variables. *Geoderma* **2023**, *429*, 116193. https://doi.org/10.1016/j.geoderma.2022.116193.
3. Cheng, M.; Zeng, G.; Huang, D.; Lai, C.; Xu, P.; Zhang, C.; Liu, Y. Hydroxyl radicals based advanced oxidation processes (AOPs) for remediation of soils contaminated with organic compounds: A review. *Chem. Eng. J.* **2016**, *284*, 582–598. https://doi.org/10.1016/j.cej.2015.09.001.
4. Aravind Kumar, J.; Krithiga, T.; Sathish, S.; Renita, A.A.; Prabu, D.; Lokesh, S.; Geetha, R.; Namasivayam, S.K.R.; Sillanpaa, M. Persistent organic pollutants in water resources: Fate, occurrence, characterization and risk analysis. *Sci. Total Environ.* **2022**, *831*, 154808. https://doi.org/10.1016/j.scitotenv.2022.154808.
5. Kampa, M.; Castanas, E. Human health effects of air pollution. *Environ. Pollut.* **2008**, *151*, 362–367. https://doi.org/10.1016/j.envpol.2007.06.012.
6. Kumar, L.; Chugh, M.; Kumar, S.; Kumar, K.; Sharma, J.; Bharadvaja, N. Remediation of petrorefinery wastewater contaminants: A review on physicochemical and bioremediation strategies. *Process Saf. Environ. Prot.* **2022**, *159*, 362–375. https://doi.org/10.1016/j.psep.2022.01.009.
7. Zhang, H.; Ma, D.; Qiu, R.; Tang, Y.; Du, C. Non-thermal plasma technology for organic contaminated soil remediation: A review. *Chem. Eng. J.* **2017**, *313*, 157–170. https://doi.org/10.1016/j.cej.2016.12.067.
8. Paria, S. Surfactant-enhanced remediation of organic contaminated soil and water. *Adv. Colloid Interface Sci.* **2008**,

138, 24–58. https://doi.org/10.1016/j.cis.2007.11.001.

9. Varjani, S.; Upasani, V.N. Influence of abiotic factors, natural attenuation, bioaugmentation and nutrient supplementation on bioremediation of petroleum crude contaminated agricultural soil. *J. Environ. Manage.* **2019**, *245*, 358–366. https://doi.org/10.1016/j.jenvman.2019.05.070.
10. Terzaghi, E.; Vergani, L.; Mapelli, F.; Borin, S.; Raspa, G.; Zanardini, E.; Morosini, C.; Anelli, S.; Nastasio, P.; Sale, V.M.; et al. New Data Set of Polychlorinated Dibenzo-p-dioxin and Dibenzofuran Half-Lives: Natural Attenuation and Rhizoremediation Using Several Common Plant Species in a Weathered Contaminated Soil. *Environ. Sci. Technol.* **2020**, *54*, 10000–10011. https://doi.org/10.1021/acs.est.0c01857.
11. Lopes, P.R.M.; Cruz, V.H.; de Menezes, A.B.; Gadanhoto, B.P.; de Almeida Moreira, B.R.; Mendes, C.R.; Mazzeo, D.E.C.; Dilarri, G.; Montagnolli, R.N. Microbial bioremediation of pesticides in agricultural soils: An integrative review on natural attenuation, bioaugmentation and biostimulation. *Rev. Environ. Sci. Bio/Technol.* **2022**, *21*, 851–876. https://doi.org/10.1007/s11157-022-09637-w.
12. Varjani, S.; Upasani, V.N.; Pandey, A. Bioremediation of oily sludge polluted soil employing a novel strain of Pseudomonas aeruginosa and phytotoxicity of petroleum hydrocarbons for seed germination. *Sci. Total Environ.* **2020**, *737*, 139766. https://doi.org/10.1016/j.scitotenv.2020.139766.
13. Mu, J.; Chen, Y.; Song, Z.; Liu, M.; Zhu, B.; Tao, H.; Bao, M.; Chen, Q. Effect of terminal electron acceptors on the anaerobic biodegradation of PAHs in marine sediments. *J. Hazard. Mater.* **2022**, *438*, 129569. https://doi.org/10.1016/j.jhazmat.2022.129569.
14. Patel, A.K.; Singhania, R.R.; Albarico, F.; Pandey, A.; Chen, C.W.; Dong, C.D. Organic wastes bioremediation and its changing prospects. *Sci. Total Environ.* **2022**, *824*, 153889. https://doi.org/10.1016/j.scitotenv.2022.153889.
15. Samaei, M.R.; Mortazavi, S.B.; Bakhshi, B.; Jafari, A.J.; Shamsedini, N.; Mehrazmay, H.; Ansarizadeh, M. Investigating the effects of combined bio-enhancement and bio-stimulation on the cleaning of hexadecane-contaminated soils. *J. Environ. Chem. Eng.* **2022**, *10*, 106914. https://doi.org/10.1016/j.jece.2021.106914.
16. Ng, Y.J.; Lim, H.R.; Khoo, K.S.; Chew, K.W.; Chan, D.J.C.; Bilal, M.; Munawaroh, H.S.H.; Show, P.L. Recent advances of biosurfactant for waste and pollution bioremediation: Substitutions of petroleum-based surfactants. *Environ. Res.* **2022**, *212*, 113126. https://doi.org/10.1016/j.envres.2022.113126.
17. Moldes, A.B.; Paradelo, R.; Rubinos, D.; Devesa-Rey, R.; Cruz, J.M.; Barral, M.T. Ex situ treatment of hydrocarbon-contaminated soil using biosurfactants from Lactobacillus pentosus. *J. Agric. Food Chem.* **2011**, *59*, 9443–9447. https://doi.org/10.1021/jf201807r.
18. Zhao, H.P.; Wang, L.; Ren, J.R.; Li, Z.; Li, M.; Gao, H.W. Isolation and characterization of phenanthrene-degrading strains *Sphingomonas* sp. ZP1 and *Tistrella* sp. ZP5. *J. Hazard. Mater.* **2008**, *152*, 1293–1300. https://doi.org/10.1016/j.jhazmat.2007.08.008.
19. Hamidi, Y.; Ataei, S.A.; Sarrafi, A. A simple, fast and low-cost method for the efficient separation of hydrocarbons from oily sludge. *J. Hazard. Mater.* **2021**, *413*, 125328. https://doi.org/10.1016/j.jhazmat.2021.125328.
20. Parera, J.; Santos, F.J.; Galceran, M.T. Microwave-assisted extraction versus Soxhlet extraction for the analysis of short-chain chlorinated alkanes in sediments. *J. Chromatogr. A* **2004**, *1046*, 19–26. https://doi.org/10.1016/j.chroma.2004.06.064.
21. Schmidt, F.; Koch, B.P.; Witt, M.; Hinrichs, K.-U. Extending the analytical window for water-soluble organic matter in sediments by aqueous Soxhlet extraction. *Geochim. Cosmochim. Acta* **2014**, *141*, 83–96. https://doi.org/10.1016/j.gca.2014.06.009.
22. Kunene, P.N.; Mahlambi, P.N. Optimization and application of ultrasonic extraction and Soxhlet extraction followed by solid phase extraction for the determination of triazine pesticides in soil and sediment. *J. Environ. Chem. Eng.* **2020**, *8*, 103665. https://doi.org/10.1016/j.jece.2020.103665.
23. Barcobonilla, N.; Vidal, J.; Garridofrenich, A.; Romerogonzalez, R. Comparison of ultrasonic and pressurized liquid extraction for the analysis of polycyclic aromatic compounds in soil samples by gas chromatography coupled to tandem mass spectrometry. *Talanta* **2009**, *78*, 156–164. https://doi.org/10.1016/j.talanta.2008.10.048.
24. Temerdashev, Z.A.; Musorina, T.N.; Chervonnaya, T.A. Determination of Polycyclic Aromatic Hydrocarbons in Soil and Bottom Sediments by Gas Chromatography–Mass Spectrometry Using Dispersive Liquid–Liquid Microextraction. *J. Anal. Chem.* **2020**, *75*, 1000–1010. https://doi.org/10.1134/s1061934820080158.
25. Li, J.; Song, X.; Hu, G.; Thring, R.W. Ultrasonic desorption of petroleum hydrocarbons from crude oil contaminated soils. *J. Environ. Sci. Health Part A* **2013**, *48*, 1378–1389. https://doi.org/10.1080/10934529.2013.781885.
26. Wu, G.; Li, X.; Coulon, F.; Li, H.; Lian, J.; Sui, H. Recycling of solvent used in a solvent extraction of petroleum hydrocarbons contaminated soil. *J. Hazard. Mater.* **2011**, *186*, 533–539. https://doi.org/10.1016/j.jhazmat.2010.11.041.
27. Ji, R.; Wu, Y.; Bian, Y.; Song, Y.; Sun, Q.; Jiang, X.; Zhang, L.; Han, J.; Cheng, H. Nitrogen-doped porous biochar

derived from marine algae for efficient solid-phase microextraction of chlorobenzenes from aqueous solution. *J. Hazard. Mater.* **2021**, *407*, 124785. https://doi.org/10.1016/j.jhazmat.2020.124785.

28. Ghiasvand, A.R.; Pirdadeh-Beiranvand, M. Cooling/heating-assisted headspace solid-phase microextraction of polycyclic aromatic hydrocarbons from contaminated soils. *Anal. Chim. Acta* **2015**, *900*, 56–66. https://doi.org/10.1016/j.aca.2015.10.016.
29. Liao, X.; Zhao, D.; Yan, X.; Huling, S.G. Identification of persulfate oxidation products of polycyclic aromatic hydrocarbon during remediation of contaminated soil. *J. Hazard. Mater.* **2014**, *276*, 26–34. https://doi.org/10.1016/j.jhazmat.2014.05.018.
30. Xu, J.; Deng, X.; Cui, Y.; Kong, F. Impact of chemical oxidation on indigenous bacteria and mobilization of nutrients and subsequent bioremediation of crude oil-contaminated soil. *J. Hazard. Mater.* **2016**, *320*, 160–168. https://doi.org/10.1016/j.jhazmat.2016.08.028.
31. Andreu, V.; Picó, Y. Pressurized liquid extraction of organic contaminants in environmental and food samples. *TrAC Trends Anal. Chem.* **2019**, *118*, 709–721. https://doi.org/10.1016/j.trac.2019.06.038.
32. Yang, Y.; Hofmann, T. Aqueous accelerated solvent extraction of native polycyclic aromatic hydrocarbons (PAHs) from carbonaceous river floodplain soils. *Environ. Pollut.* **2009**, *157*, 2604–2609. https://doi.org/10.1016/j.envpol.2009.05.020.
33. Yin, H.; Tan, Q.; Chen, Y.; Lv, G.; Hou, X. Polycyclic aromatic hydrocarbons (PAHs) pollution recorded in annual rings of gingko (*Gingko biloba* L.): Determination of PAHs by GC/MS after accelerated solvent extraction. *Microchem. J.* **2011**, *97*, 138–143. https://doi.org/10.1016/j.microc.2010.08.008.
34. Humbert, K.; Debret, M.; Morin, C.; Cosme, J.; Portet-Koltalo, F. Direct thermal desorption-gas chromatography-tandem mass spectrometry versus microwave assisted extraction and GC-MS for the simultaneous analysis of polyaromatic hydrocarbons (PAHs, PCBs) from sediments. *Talanta* **2022**, *250*, 123735. https://doi.org/10.1016/j.talanta.2022.123735.
35. Sanchez-Prado, L.; Garcia-Jares, C.; Dagnac, T.; Llompart, M. Microwave-assisted extraction of emerging pollutants in environmental and biological samples before chromatographic determination. *TrAC Trends Anal. Chem.* **2015**, *71*, 119–143. https://doi.org/10.1016/j.trac.2015.03.014.
36. Humbert, K.; Debret, M.; Morin, C.; Cosme, J.; Portet-Koltalo, F. Direct thermal desorption-gas chromatography-tandem mass spectrometry versus microwave assisted extraction and GC-MS for the simultaneous analysis of polyaromatic hydrocarbons (PAHs, PCBs) from sediments. *Talanta* **2022**, *250*, 123735. https://doi.org/10.1016/j.talanta.2022.123735.
37. Gallo, M.; Ferrara, L.; Naviglio, D. Application of Ultrasound in Food Science and Technology: A Perspective. *Foods* **2018**, *7*, 164.https://doi.org/10.3390/foods7100164.
38. Zhang, H.; Zhao, J.; Shang, H.; Guo, Y.; Chen, S. Extraction, purification, hypoglycemic and antioxidant activities of red clover (*Trifolium pratense* L.) polysaccharides. *Int. J. Biol. Macromol.* **2020**, *148*, 750–760. https://doi.org/10.1016/j.ijbiomac.2020.01.194
39. Karmakar, B.; Saha, S.P.; Chakraborty, R.; Roy, S. Optimization of starch extraction from Amorphophallus paeoniifolius corms using response surface methodology (RSM) and artificial neural network (ANN) for improving yield with tenable chemical attributes. *Int. J. Biol. Macromol.* **2023**, *237*, 124183. https://doi.org/10.1016/j.ijbiomac.2023.124183
40. Wang, X.; Liu, X.; Shi, N.; Zhang, Z.; Chen, Y.; Yan, M.; Li, Y. Response surface methodology optimization and HPLC-ESI-QTOF-MS/MS analysis on ultrasonic-assisted extraction of phenolic compounds from okra (Abelmoschus esculentus) and their antioxidant activity. *Food Chem.* **2023**, *405*, 134966. https://doi.org/10.1016/j.foodchem.2022.134966
41. Chapman, J.; Truong, V.K.; Elbourne, A.; Gangadoo, S.; Cheeseman, S.; Rajapaksha, P.; Latham, K.; Crawford, R.J.; Cozzolino, D. Combining Chemometrics and Sensors: Toward New Applications in Monitoring and Environmental Analysis. *Chem. Rev.* **2020**, *120*, 6048–6069. https://doi.org/10.1021/acs.chemrev.9b00616.
42. dos Santos, P.N.A.; Conrado, T.M.; Neubauer, A.L.; dos Santos, L.C.; Krause, E.B. Caramão, Optimization of Energized Dispersive Guided extraction (EDGE) of antioxidants from *Eugenia uniflora* L. (Pitanga) leaves using response surface methodology. *Microchem. J.* **2023**, *187*, 108411. https://doi.org/10.1016/j.microc.2023.108411.
43. Luo, X.; Gong, H.; He, Z.; Zhang, P.; He, L. Recent advances in applications of power ultrasound for petroleum industry. *Ultrason. Sonochem.* **2021**, *70*, 105337. https://doi.org/10.1016/j.ultsonch.2020.105337.
44. Rao, M.V.; Sengar, A.S.; Sunil, C.K.; Rawson, A. Ultrasonication—A green technology extraction technique for spices: A review. *Trends Food Sci. Technol.* **2021**, *116*, 975–991. https://doi.org/10.1016/j.tifs.2021.09.006.
45. Hafidi, M.; Amir, S.; Jouraiphy, A.; Winterton, P.; El Gharous, M.; Merlina, G.; Revel, J.C. Fate of polycyclic aromatic

hydrocarbons during composting of activated sewage sludge with green waste. *Bioresour. Technol.* **2008**, *99*, 8819–8823. https://doi.org/10.1016/j.biortech.2008.04.044.

46. Liu, T.; Li, W.; Li, L.; Peng, X.; Kuang, T. Effect of dynamic oscillation shear flow intensity on the mechanical and morphological properties of high-density polyethylene: An integrated experimental and molecular dynamics simulation study. *Polym. Test.* **2019**, *80*, 106122. https://doi.org/10.1016/j.polymertesting.2019.106122.
47. Chen, G.; Xu, R.; Zhang, C.; Lv, Y. Responses of MSCs to 3D Scaffold Matrix Mechanical Properties under Oscillatory Perfusion Culture. *ACS Appl. Mater. Interfaces* **2017**, *9*, 1207–1218. https://doi.org/10.1021/acsami.6b10745.
48. Deng, Y.; Wang, W.; Zhao, S.; Yang, X.; Xu, W.; Guo, M.; Xu, E.; Ding, T.; Ye, X.; Liu, D. Ultrasound-assisted extraction of lipids as food components: Mechanism, solvent, feedstock, quality evaluation and coupled technologies—A review. *Trends Food Sci. Technol.* **2022**, *122*, 83–96. https://doi.org/10.1016/j.tifs.2022.01.034.
49. Avvaru, B.; Venkateswaran, N.; Uppara, P.; Iyengar, S.B.; Katti, S.S. Current knowledge and potential applications of cavitation technologies for the petroleum industry. *Ultrason. Sonochem.* **2018**, *42*, 493–507. https://doi.org/10.1016/j.ultsonch.2017.12.010.
50. Khadhraoui, B.; Ummat, V.; Tiwari, B.K.; Fabiano-Tixier, A.S.; Chemat, F. Review of ultrasound combinations with hybrid and innovative techniques for extraction and processing of food and natural products. *Ultrason. Sonochem.* **2021**, *76*, 105625. https://doi.org/10.1016/j.ultsonch.2021.105625.
51. Jha, A.K.; Sit, N. Extraction of bioactive compounds from plant materials using combination of various novel methods: A review. *Trends Food Sci. Technol.* **2022**, *119*, 579–591. https://doi.org/10.1016/j.tifs.2021.11.019.
52. Wang, J.; Yang, Z.; Zhou, X.; Waigi, M.G.; Gudda, F.O.; Odinga, E.S.; Mosa, A.; Ling, W. Nitrogen addition enhanced the polycyclic aromatic hydrocarbons dissipation through increasing the abundance of related degrading genes in the soils. *J. Hazard. Mater.* **2022**, *435*, 129034. https://doi.org/10.1016/j.jhazmat.2022.129034.
53. Teng, Y.; Luo, Y.; Ping, L.; Zou, D.; Li, Z.; Christie, P. Effects of soil amendment with different carbon sources and other factors on the bioremediation of an aged PAH-contaminated soil. *Biodegradation* **2010**, *21*, 167–178. https://doi.org/10.1007/s10532-009-9291-x.
54. Badr, T.; Hanna, K.; de Brauer, C. Enhanced solubilization and removal of naphthalene and phenanthrene by cyclodextrins from two contaminated soils. *J. Hazard. Mater.* **2004**, *112*, 215–223. https://doi.org/10.1016/j.jhazmat.2004.04.017.
55. Yao, Y.; Huang, G.H.; An, C.J.; Cheng, G.H.; Wei, J. Effects of freeze-thawing cycles on desorption behaviors of PAH-contaminated soil in the presence of a biosurfactant: A case study in western Canada. *Environ. Sci. Process. Impacts* **2017**, *19*, 874–882. https://doi.org/10.1039/c7em00084g.
56. Lin, W.; Liu, S.; Tong, L.; Zhang, Y.; Yang, J.; Liu, W.; Guo, C.; Xie, Y.; Lu, G.; Dang, Z. Effects of rhamnolipids on the cell surface characteristics of *Sphingomonas* sp. GY2B and the biodegradation of phenanthrene. *RSC Adv.* **2017**, *7*, 24321–24330. https://doi.org/10.1039/c7ra02576a.
57. Johann, S.; Seiler, T.B.; Tiso, T.; Bluhm, K.; Blank, L.M.; Hollert, H. Mechanism-specific and whole-organism ecotoxicity of mono-rhamnolipids. *Sci. Total Environ.* **2016**, 548–549, 155–163. https://doi.org/10.1016/j.scitotenv.2016.01.066.
58. Techer, D.; Laval-Gilly, P.; Henry, S.; Bennasroune, A.; Formanek, P.; Martinez-Chois, C.; D'Innocenzo, M.; Muanda, F.; Dicko, A.; Rejsek, K.; et al. Contribution of Miscanthus x giganteus root exudates to the biostimulation of PAH degradation: An in vitro study. *Sci. Total Environ.* **2011**, *409*, 4489–4495. https://doi.org/10.1016/j.scitotenv.2011.06.049.
59. Xiang, L.; Harindintwali, J.D.; Wang, F.; Redmile-Gordon, M.; Chang, S.X.; Fu, Y.; He, C.; Muhoza, B.; Brahushi, F.; Bolan, N.; et al. Integrating Biochar, Bacteria, and Plants for Sustainable Remediation of Soils Contaminated with Organic Pollutants. *Environ. Sci. Technol.* **2022**, *56*, 16546–16566. https://doi.org/10.1021/acs.est.2c02976.
60. Chen, Y.; Zhao, Z.; Peng, Y.; Li, J.; Xiao, L.; Yang, L. Performance of a full-scale modified anaerobic/anoxic/oxic process: High-throughput sequence analysis of its microbial structures and their community functions. *Bioresour. Technol.* **2016**, *220*, 225–232. https://doi.org/10.1016/j.biortech.2016.07.095.
61. Yang, S.; Zhao, L.; Chang, X.; Pan, Z.; Zhou, B.; Sun, Y.; Li, X.; Weng, L.; Li, Y. Removal of chlortetracycline and antibiotic resistance genes in soil by earthworms (epigeic Eisenia fetida and endogeic Metaphire guillelmi). *Sci. Total Environ.* **2021**, *781*, 146679. https://doi.org/10.1016/j.scitotenv.2021.146679.
62. Li, J.; Luo, C.; Song, M.; Dai, Q.; Jiang, L.; Zhang, D.; Zhang, G. Biodegradation of Phenanthrene in Polycyclic Aromatic Hydrocarbon-Contaminated Wastewater Revealed by Coupling Cultivation-Dependent and -Independent Approaches. *Environ. Sci. Technol.* **2017**, *51*, 3391–3401. https://doi.org/10.1021/acs.est.6b04366.
63. Wang, C.; Huang, Y.; Zhang, Z.; Hao, H.; Wang, H. Absence of the nahG-like gene caused the syntrophic interaction between Marinobacter and other microbes in PAH-degrading process. *J. Hazard. Mater.* **2020**, *384*, 121387.

https://doi.org/10.1016/j.jhazmat.2019.121387.

64. Cui, Z.; Xu, G.; Gao, W.; Li, Q.; Yang, B.; Yang, G.; Zheng, L. Isolation and characterization of Cycloclasticus strains from Yellow Sea sediments and biodegradation of pyrene and fluoranthene by their syntrophic association with Marinobacter strains. *Int. Biodeterior. Biodegrad.* **2014**, *91*, 45–51. https://doi.org/10.1016/j.ibiod.2014.03.005.
65. Shi, J.; Jiang, J.; Chen, Q.; Wang, L.; Nian, K.; Long, T. Production of higher toxic intermediates of organic pollutants during chemical oxidation processes: A review. *Arabian J. Chem.* **2023**, *16*, 104856. https://doi.org/10.1016/j.arabjc.2023.104856.
66. Ma, L.; Cai, Q.; Ong, S.L.; Yang, Z.; Zhao, W.; Duan, J.; Hu, J. Photonic efficiency optimization-oriented dependence model of characteristic coupling spectrum on catalytic absorbance in photocatalytic degradation of tetracycline hydrochloride. *Chem. Eng. J.* **2023**, *451*, 138623. https://doi.org/10.1016/j.cej.2022.138623.
67. Tian, H.; Peng, S.; Zhao, L.; Chen, Y.; Cui, K. Simultaneous adsorption of Cd(II) and degradation of OTC by activated biochar with ferrate: Efficiency and mechanism. *J. Hazard. Mater.* **2023**, *447*, 130711. https://doi.org/10.1016/j.jhazmat.2022.130711.